

# ELECTROCHEMICAL INVESTIGATION OF $Y_xZr_{1-x}Mn_mFe_nCo_pV_oCr_q(m+n+o+p+q=2)$ ELECTRODE FOR Ni-MH BATTERY APPLICATION

N.Rajalakshmi, K.S.Dhathathreyan  
 Centre for Electrochemical and Energy Research  
 SPIC Science Foundation  
 111, Mount Road  
 Guindy, Chennai 600 032, INDIA  
 &  
 Sundara Ramaprabhu  
 Magnetism and Magnetic Materials Laboratory  
 Department of Physics  
 Indian Institute of Technology  
 Chennai 600 036, INDIA

## ABSTRACT:

The  $AB_2$  type Laves phase hydrogen absorbing alloys are being investigated as suitable electrode materials for Ni-MH batteries, because of their higher electrochemical capacity. The electrochemical properties like electrode potential, reversible electrochemical capacity and diffusion coefficient as a function of state of charge in the  $Y_xZr_{1-x}Mn_mFe_nCo_pV_oCr_q(m+n+o+p+q=2)$  electrodes were investigated in an alkaline solution. The reversible electrochemical capacity of the electrode was found to be in excess of 450 mAh/g and hydrogen concentration was estimated as 3.5 hydrogens/formula unit. The process that occur in the electrode during charge and discharge, has been studied by Cyclic Voltammogram(CV) experiments, carried out at different sweep rates. It was found that at low sweep rates, the hydrogen concentration on the surface increases due to longer polarisation and the hydrogen concentration approaches a value which favours a metal hydride formation. The diffusion coefficients were also evaluated with respect to state of charge. The results will be presented in the paper.

## INTRODUCTION:

$AB_2$  hydrogen storage alloys are promising for negative electrodes in Ni-MH batteries for their higher discharge capacities and better resistance to oxidation than those of  $AB_5$  alloys[1,2]. As  $AB_2$  type multiphase hydrogen storage alloys are mainly composed of C14, C15 Laves phase, and some solid solutions with bcc structure, there exist abundant boundaries, with enriched electrochemically catalytic elements as active reaction sites and diffusion pipes for transporting reactants and products. However, the activation and electro-catalytic activity of the alloy electrode is still inferior to that of the  $MmNi_5$  based alloy [3]. The main reasons for the slow activation and low electro-catalytic activity are: an oxide layer is formed on the surface of the alloy grains, and this oxide layer is a bad electrical conductor, hence impedes the diffusion of hydrogen and absence of Ni content layer on these  $AB_2$  alloy surface results in a lower surface activity for hydrogen absorption/desorption [4].

The hydrogen storage properties of the alloys, whether as an electrode or as a storage medium, are initially related to their composition and vary widely with small changes in the type and the amount of substituent elements[5]. Thus, depending on the battery use, it is possible to design the electrode characteristics by changing the alloy compositions. The choice of the material is based on the desirable metal-hydrogen bond strength for use as electrodes in aqueous media and an appreciable hydrogen storage capacity/partial substitution for both the A and B sites, dramatically improves the cycle lifetime and the electrochemical discharge capacity has been optimized by substituting various metals as partial constituents, and by moving the composition ratio from stoichiometry. This has resulted in the preparation of four or five component Laves phase hydrogen storage alloys with discharge capacities over 400 mAh/g[ 6]. Knosp et al [7] have studied the Laves phase alloys of composition  $(Zr,Ti)(Ni,Mn,M)_x$  where  $M = Cr, V, Co, Al$  and  $x = 1.9$  to 2.1 with hexagonal C14 or cubic C15 structure in order to select the most suitable  $AB_2$  alloys as an active material for Ni-MH batteries. Kim et al [8] studied the hydrogen storage performance and electrochemical properties of  $ZrMn_{1-x}V_xNi_{1.4+y}$  ( $x = 0.5, 0.7$ ;  $y =$

0.0 to 0.6) and found that the major factor controlling the electrode properties was the specific reaction surface area and the exchange current density depending upon the composition. The maximum electrochemical capacity experimentally observed was found to be 338 mAh/g for  $ZrMn_{0.5}V_{0.5}Ni_{1.4}$ , and the discharge efficiency was found to be 85%. Hence fundamental studies on the charge/discharge characteristics are required for improving the performance of a Ni-MH battery [9,10]. The present work focuses on elucidating the electrochemical properties like charge/discharge characteristics, diffusion coefficient etc., or an  $AB_2$  compound with the composition  $Y_xZr_{1-x}Mn_mFe_nCo_pV_oCr_q(m+n+o+p+q=2)$  and the processes that occur during charge and discharge were also evaluated.

## EXPERIMENTAL:

Hydrogen storage alloys of composition  $Y_xZr_{1-x}Mn_mFe_nCo_pV_oCr_q(m+n+o+p+q=2)$  were prepared by arc melting in an argon atmosphere. The buttons were turned upside down and remelted 5 to 6 times in order to get good homogeneity and the alloy buttons were annealed at 900 K for about 3 days. The intermetallics were pulverized mechanically into powders in an agate mortar. Structure and phase density of the sample was characterized by X-ray diffraction (XRD). The samples prepared had an overall  $AB_2$  phase.

For the electrochemical measurements, the electrodes were prepared by grinding the alloy into 75  $\mu$  size and mixing it with copper powder in the ratio of 1:3 with a PTFE binder. The putty form of the mixture was mechanically pressed onto a current collector (Ni mesh) at RT. Then the electrode was sintered at 300°C for about 3 hrs under vacuum. The geometric area of the electrode was about 2 cm<sup>2</sup>. The counter electrode was Pt, has a much larger geometric area than the WE. The electrolyte 31% KOH, which is the same as that used in the alkaline batteries, were prepared from reagent grade KOH and deionised water. The electrodes were tested for their charge-discharge characteristics, initial capacity, cycle life and diffusion coefficient. The electrochemical measurements were carried out in a flooded electrolyte condition in open cells. Potentials were monitored using a saturated calomel as reference electrode. The electrochemical measurements include the diffusion coefficient as a function of state of charge and also the electrochemical processes that occur during charge/discharge. These measurements were carried out using a EG & G galvanostat/potentiostat Model 273, with the available techniques like chronopotentiometry, cyclic voltammetry and constant potential coulometry.

## RESULTS AND DISCUSSION:

The electrochemical capacity of a hydride electrode depends on the amount of reversibly absorbed hydrogen in the hydriding material. Fig. 1 shows the charge/discharge curves of the electrode after 30 cycles. The electrode showed the highest electrochemical charging capacity of 470 mAh/g, which corresponds to a hydrogen concentration of 3.5 hydrogens/formula unit. Hydrogen evolution was found to occur around -1.35V. This shows that the metal-hydrogen bond is not weak, and hence hydrogen can react with the alloy for hydride formation. However, if the bond is very strong, the metal hydride electrode is extensively oxidised, and cannot store hydrogen reversibly. The coulombic efficiency was found to be 85%, the charging potential and the discharging potential was around -0.9 and -0.5V respectively. The electrochemical charging capacity was found to be slightly lower when the electrode is charged at the 2C rate (80 mA) compared to the 1C rate (40 mA) as shown in Fig 2. As already mentioned, the highest electrochemical capacity was observed only after 30 cycles and then the capacity remained constant for almost 100 cycles, as shown in Fig.3, which clearly reveals that degradation of the electrode material is very slow.

To estimate the diffusion coefficient parameter  $D/a^2$ , the following procedure was carried out. The alloy was fully activated by charging and discharging the electrode for about 30 cycles. Then the electrodes with different states of charge were equilibrated until an equilibrium potential was reached. Initially, the activated electrode was discharged at constant potential at three different states of charge. In order to secure a zero concentration of hydrogen at the surface of each individual particle, the electrode was

discharged at a constant anodic potential of  $-0.56\text{V}(\text{SCE})$ . Discharge curves obtained for seven different charged states are given in Fig. 4. For large times in Fig.4, an approximately a linear relationship exists between  $\log(i)$  and  $t$ , which is consistent with the equation

$$\log(i) = \log\{(6FD(C_0 - C_s)/da^2) - (\pi^2/2.303)(D/a^2)t\} \quad (1)$$

Where  $C_0$  is the concentration in the bulk of the alloy and a constant surface concentration  $C_s$ ,  $\pm$  sign indicates the charge (-) and discharge (+) process [11]. From the slope of the linear portion of the corresponding curves in Fig.4, the ratios of  $D/a^2$  were estimated.

The diffusion coefficient may also be determined from the amount of charge transferred [12]. Assuming that the hydride alloy particles are in spherical form, the diffusion equation is,

$$\partial(rc)/\partial t = D \partial^2(rc)/\partial r^2 \quad (2)$$

where  $c$  is the concentration of hydrogen in the alloy,  $t$  is the time,  $D$  is an average(or integral) diffusion coefficient of hydrogen over a defined concentration range, and  $r$  is a distance from the centre of the sphere. Since the discharge process was carried out under a constant current condition, it is reasonable to assume that a constant flux of the species at the surface and uniform initial concentration of hydrogen in the bulk of the alloy. Thus, the value of  $D/a^2$  may be evaluated for large transition times,  $\tau$ ,

$$D/a^2 = 1/[15\{Q_0/I - \tau\}] \quad (3)$$

Where  $Q_0$  is the initial specific capacity (c/g),  $I$  is the current density (A/g) and  $\tau$  is the transient time (s), i.e the time required for the hydrogen surface concentration to become zero. The ratio  $Q_0/I$  corresponds to the discharge time necessary to discharge completely the electrode under hypothetical conditions, when the process proceeds without the interference of diffusion. Thus  $D/a^2$  were calculated using the above equation for different states of charge and are given in Fig.5. As shown in Fig.5, the ratio of  $D/a^2$  is almost independent of the state of charge with an average value of  $0.37 \times 10^{-5} \text{ s}^{-1}$ . Assuming that the average particle radius is  $15 \mu\text{m}$ , the effective diffusion coefficient of hydrogen through the  $\text{Y}_x\text{Zr}_{1-x}\text{Mn}_m\text{Fe}_n\text{Co}_p\text{V}_o\text{Cr}_q(m+n+o+p+q=2)$  electrode was estimated to be  $8.32 \times 10^{-12} \text{ cm}^2/\text{s}$ . This value is in consistent with the diffusion coefficient of hydrogen in Nickel alloys, which are in the range  $20 \times 10^{-12}$  to  $56 \times 10^{-12} \text{ cm}^2/\text{s}$  estimated using a permeation technique[13-15]. Fig 6 shows the cyclic voltammogram(CV) of an activated sample of the alloy after 5 cycles ranging from  $-0.6$  to  $-1.4 \text{ v}$  vs SCE at various scanning rates. The definite peaks at potentials ranging from  $-0.9$  to  $-1.2 \text{ v}$  were observed and these adsorption peaks indicate that there are H atoms adsorbed on the surface due to the formation of the hydride. The counterparts responsible for the desorption of hydrogen from the alloys were also observed and are shown in Fig 7 in the range  $-0.1$  to  $-0.6$ . At low sweep rates, the hydrogen concentration on the surface increases due to longer polarisation and the hydrogen concentration approaches a value for the hydride formation.

#### ACKNOWLEDGEMENTS:

The authors are thankful to the Management, SPIC Science Foundation, for the financial assistance and for the facilities provided to carry out this work.

## REFERENCES:

1. S.R.Ovshinsky, M.A.Fetcenko, J.Ross, Science, 260(91)(1990), 176
2. X.L.Wang, S.Suda, S.Wakao, Z.Phys.Chem 183(1994), 297
3. H.Sawa, S.Wakao, Mater.Trans JIM, 31 (1990)487
4. A.Züttel, F.McLi and L.Schlapbach, J Alloys and Compounds 231(1995) 645
5. T.Sakai, K.Oguro, H.Miyamura, N.Kuriyama, A.Kato, H.Ishikawa and K.Iwakura, J Less Common Metals 231(1995) 645
6. H.Nakano, I.Wada and S. Wakao, Denki Kagaku, 672 (1994) 953
7. B.Knosp, C.Jordy, Ph.Blanchard and T.Berlureau, J Electrochem soc 145, (1998) 1478
8. Dong-Myung Kim, Sang-Min Lee, Jae-Han Jung, Kuk-Jin Jang and Jai-Young Lee, J Electrochem Soc 145(1998) 93
9. H.Inoue, K.Yamataka, Y.Fukumoto and C.Iwakura, J Electrochem Soc 143(1996) 2527
10. M.P.Sridhar Kumar, W.Zhang, K.Petrov, A.A. Rostami and S.Srinivasan, J Electrochem soc 142 (1995) 3424
11. G.Zheng, B.N.Popov and R.E White, J.Electrochem Soc 142(1995) 2695
12. G.Zheng, B.N.Popov and R.E White, J.Electrochem Soc 143(1996) 834
13. W.M.Robertson, Metall Trans., 8A, (1977) 1709
14. R.M.Latanision and M.Kurkela, Corrosion, 39,(1983), 174
15. W.M.Robertson, Metall Trans., 10A, (1979) 489

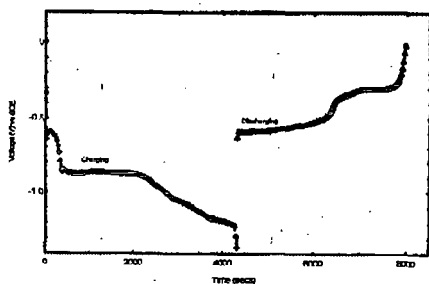


Fig. 1. Charge-Discharge characteristics of the electrode at 1C rate

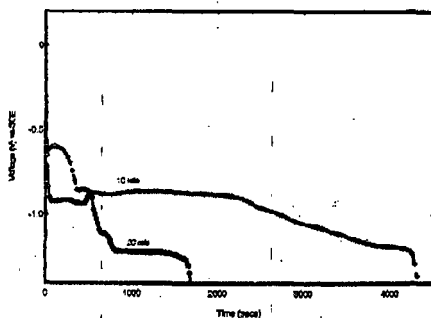


Fig.2 Capacity dependence with different charging rates

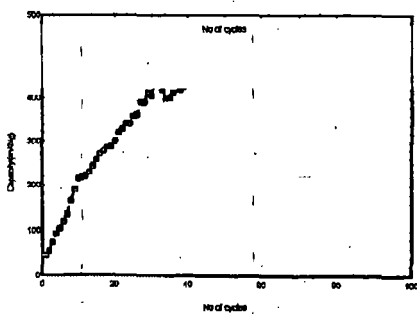


Fig. 3 Capacity variation with Cycle Number

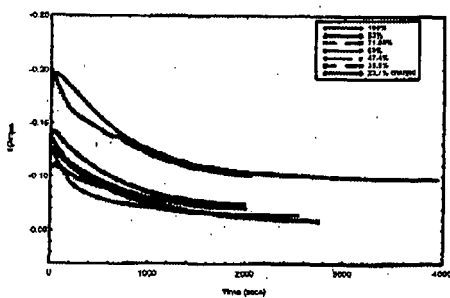


Fig. 4 Constant potential discharge curves at different states of charge

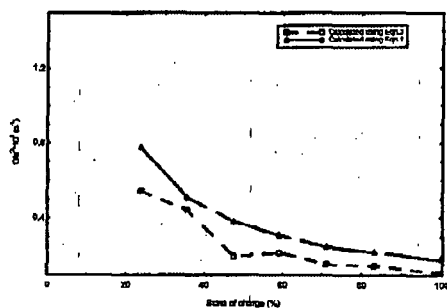


Fig. 5 Dependence of Diffusion coefficient with state of charge

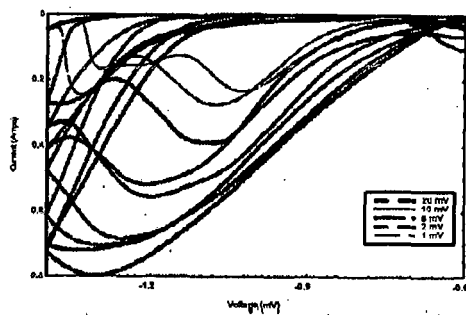


Fig. 6 Cyclic Voltammogram(CV) of the electrode for absorption at various sweep rates

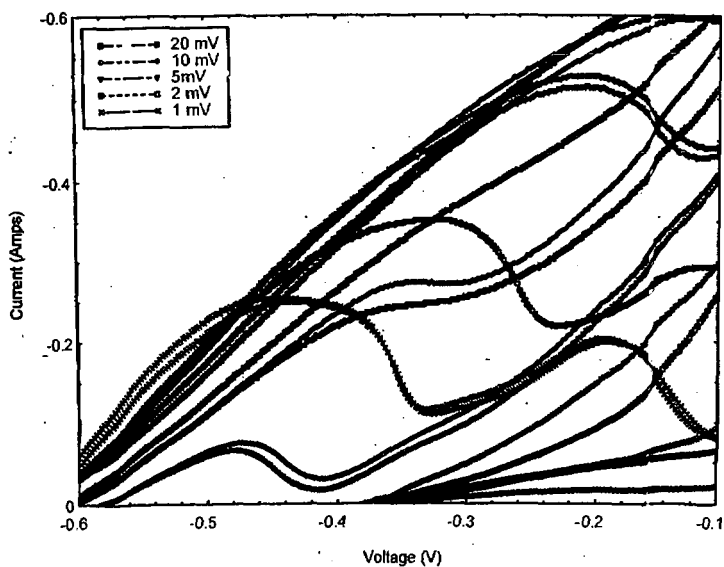


Fig. 7 Cyclic Voltammogram(CV) of the electrode for desorption at various sweep rates